

## Quantitative Study of Magnetization Reversal by Spin-Polarized Current in Magnetic Multilayer Nanopillars

F. J. Albert, N. C. Emley, E. B. Myers, D. C. Ralph, and R. A. Buhrman

*Cornell University, Ithaca, New York 14853-2501*

(Received 17 July 2002; published 6 November 2002)

We have studied magnetic switching by spin-polarized currents and also the magnetoresistance in sub-100-nm-diam thin-film Co/Cu/Co nanostructures, with the current flowing perpendicular to the plane of the films. By independently varying the thickness of all three layers and measuring the change of the switching currents, we test the theoretical models for spin-transfer switching. In addition, the changes in the switching current and magnetoresistance as a function of the Cu layer thickness give two independent measurements of the room-temperature spin-diffusion length in Cu.

DOI: 10.1103/PhysRevLett.89.226802

PACS numbers: 73.40.-c, 75.60.Jk, 75.70.Pa

The recent prediction [1–8] and demonstration of both spin-polarized current driven hysteretic switching of the magnetic orientation of a thin-film nanomagnet [9–14] and measurements consistent with direct current excitation of spin waves [10,11,13–15] have stimulated widespread interest in these new “spin-transfer” phenomena. These effects are of fundamental interest because of the insights their study can provide into spin transport and magnetic behavior at the nanoscale and are of technological importance because they offer the possibility of a new class of spin-electronic devices, including a current-switched, rather than a magnetic-field-switched, nanoscale magnetic memory element. While the possibility of achieving spin-transfer effects in nanoscale magnetic systems has now been established, the theoretical understanding is still evolving, and we are only at the initial stages of exploiting these effects for nanomagnetics and spin-transport research and of optimizing them for possible applications.

Here we present a study of spin-transfer switching and spin transport in magnetic nanopillar devices in which the device geometry has been varied over a substantial range. This has enabled quantitative measurements that determine whether spin transfer occurs predominantly at the surface of the nanomagnet or in its interior and that test the applicability of alternative “effective field” and “spin-torque” models of the spin-transfer effect. These experiments have also yielded an accurate determination of the room-temperature (RT) magnetoresistance (MR) of Co-Cu-Co trilayers in the current-perpendicular-to-the-plane (CPP) geometry, a subject of continuing theoretical interest, and a RT measurement of the spin-relaxation length  $\lambda_s$  in Cu, a key parameter for future spin-transfer device design.

We fabricated these spin-transfer devices by first sputtering a Cu (80 nm)/Co ( $t_{\text{Fixed}}$  nm)/Cu ( $d_{\text{Cu}}$  nm)/Co ( $t_{\text{Free}}$  nm)/Au (10 nm) multilayer onto an oxidized Si substrate, where we varied  $t_{\text{Fixed}}$ ,  $d_{\text{Cu}}$ , and  $t_{\text{Free}}$  to observe the dependence of the spin-transfer effect on the thickness of the magnetic layers and the spacer layer.

The 80 nm Cu base layer served as the bottom electrode and the bottom Co layer served as the fixed ferromagnet and spin polarization source, with  $t_{\text{Fixed}} \geq 4t_{\text{Free}}$ . The nanopillar devices were patterned into these multilayer films by electron beam lithography, thermal evaporation of a metal mask, and ion milling as reported previously [11,12]. A variety of shapes (circles, ellipses, elongated hexagons) and a range of lateral dimensions (60 to 150 nm) were fabricated to investigate the spin-transfer switching behavior. Within this size range, the upper limit of which is set to avoid any significant self-field effects [16,17], sample fabrication resulted in devices that varied  $\pm 5$  nm across a wafer, giving us our dominant experimental uncertainty. In some cases the bottom, thicker Co layer was left unpatterned. This has the advantage of reducing magnetic coupling between the edge charges of the fixed layer and the free layer nanomagnet [12,18].

The differential resistance  $dV/dI$  versus the applied magnetic field  $H$  of a representative  $60 \times 180$  nm elliptical Co/Cu/Co nanopillar device is shown in Fig. 1(a) for one complete cycle of  $H$  from zero to  $\pm 1200$  Oe and back at RT. Here  $t_{\text{Fixed}} = 8$  nm,  $d_{\text{Cu}} = 6$  nm, and  $t_{\text{Free}} = 2$  nm. For each pass of  $H$  through zero, the nanopillar switches to the antiparallel state at a low field and then back to the parallel state at high field, resulting in a differential resistance change  $\Delta R = 57$  m $\Omega$ . Averaging over a number of samples, all having a 2 nm thick free Co layer but varying cross-sectional area  $A$  and shape, we determined that the RT  $\Delta RA = 0.48 \pm 0.02$  m $\Omega$ - $\mu\text{m}^2$  for nanopillar devices that exhibit low  $R$  and high  $\Delta R$ . The majority of the uncertainty in this result arises from the determination of  $A$ . Substantially higher or lower values of  $\Delta RA$  were sometimes observed. Such deviations were correlated with a device resistance  $R$  that is either anomalously high, indicative of high contact resistance at the top of the nanopillar, or anomalously low, indicative of partial electrical shorting of the magnetic layers in the nanopillar due to a processing problem. The value of  $\Delta RA$  for good devices is quite close to the prediction of  $\Delta RA = 0.44$  m $\Omega$ - $\mu\text{m}^2$ , obtained from a simple ballistic model

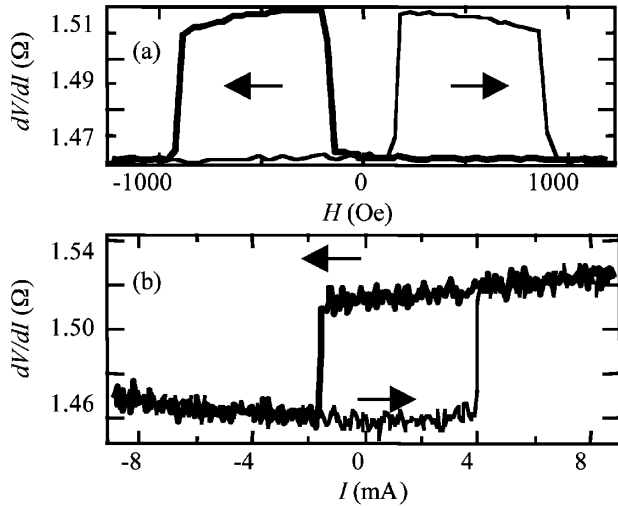


FIG. 1. (a)  $dV/dI$  of a nanopillar spin-transfer device (with parameters given in the text) as a function of the applied field. (b)  $dV/dI$  of the device as a function of the applied current. For positive  $I$ , electrons flow from the thin to the thick Co film.

that uses the spin-dependent transmissivity probabilities of Cu/Co interfaces determined by Andreev reflection measurements,  $T_{\uparrow} = 0.96$ ,  $T_{\downarrow} = 0.57$  [19], and also to the prediction  $\Delta RA = 0.53 \text{ m}\Omega\text{-}\mu\text{m}^2$  [5,6], from a Boltzmann equation calculation that used spin-dependent transport parameters, including  $T_{\uparrow} = 0.949$ ,  $T_{\downarrow} = 0.607$ , extracted from much larger area Co-Cu multilayer CPP MR measurements [20].

MR measurements were also made for nanopillar samples with free layer thicknesses of 1.2, 3.6, and 6.0 nm. For these samples, we found  $\Delta RA = 0.45 \pm 0.08 \text{ m}\Omega\text{-}\mu\text{m}^2$  with no significant variation being observed between devices of different free layer thickness. This constancy of  $\Delta RA$  supports the viewpoint that the MR of Co/Cu/Co nanopillar structures, in this thickness range, is dominated by spin-dependent interfacial scattering, either specular or diffuse, that arises from the electronic structure differences of the Co and Cu layers [20–23].

In Fig. 1(b) we show the  $dV/dI$  response versus bias current  $I$  of the device of Fig. 1(a) for one complete cycle of the current from zero to  $\pm 9$  mA. Consistent with previous results [9–13], the transfer of spin momentum to the thin (free) Co layer by the electrons flowing from the thick (fixed) Co layer forces the nanomagnet into parallel alignment (low-resistance state) at large negative currents, beyond a critical-current density  $J_c^-$ . When the electrons flow from the free layer, above a critical-current density  $J_c^+$  the device is switched back into antiparallel alignment (high-resistance state) with the Co layer. The  $\Delta R$  measured with spin-transfer switching is identical to the  $\Delta R$  measured with the field scan. In general, we find that, within the nanopillar size range of this study, devices which show the well-separated, rather abrupt magnetic switching behavior illustrated in Fig. 1(a) also

exhibit similarly abrupt spin-transfer behavior as illustrated in Fig. 1(b). For larger diameter nanopillars,  $\approx 120$  nm, multiple steps are sometimes observed in the  $R(H)$  scans, indicative of metastable domain formation in both the thin and thick Co layers. The spin-transfer switching of such devices also generally proceeds in a stepwise behavior.

To further quantify the spin-transfer effect and to test recent model calculations,  $J_c$  was measured for a variety of sample shapes and sizes, with  $t_{\text{Free}}$  ranging between 1.2 and 6.0 nm and fixed layer thickness from 8.0 to 40.0 nm. Samples with  $t_{\text{Free}} = 10$  nm were also fabricated, but a clear hysteretic switching behavior was not observed with those, most likely due to self-field effects from the large currents necessary to reorient the magnet. Process and geometry variations resulted in a range of dipolar coupling fields, causing  $J_c^+$  and  $J_c^-$  to vary by  $\leq 20\%$ ; however, we found that the quantity  $\Delta J_c \equiv J_c^+ - J_c^-$  varied by no more than 10% from sample to sample. In Fig. 2 we show the average value of  $\Delta J_c$  for five different values of  $t_{\text{Free}}$ . The sizes of these devices ranged between 0.005 and 0.013  $\mu\text{m}^2$ . As shown in Fig. 2, the measured critical-current densities between 1.2 and 6.0 nm closely follow a linear behavior, with  $\Delta J_c = 3.2 \pm 0.2 \times 10^7 \text{ A/cm}^2 \times t_{\text{Free}}/\text{nm}$  for a dc current ramp of 0.1 mA/sec.

Because of the small size of these magnetic nanostructures, thermal fluctuations play a substantial role in their switching behavior. Our group has recently reported the study of such effects on both the magnetic and spin-transfer switching of similar nanopillar samples [24], which can be described in terms of activated transitions over an energy barrier [25–27]. As result of these thermal fluctuations, the critical current  $\bar{I}_c$  measured

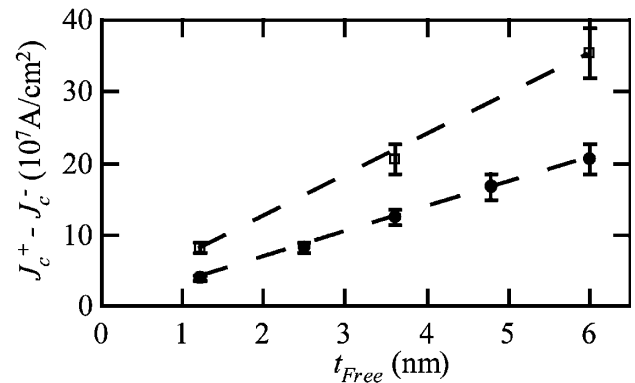


FIG. 2. Critical current density,  $\Delta J_c \equiv J_c^+ - J_c^-$ , as a function of the thickness of the spin-transfer layer for a current ramp rate of 300 mA/sec (open squares) and 0.1 mA/sec (closed circles). The dashed lines are guides to the eye. The data point for each thickness represents the measurement of the average critical current of four to ten different samples of that thickness, measured in zero field, with the error bars representing both the sample to sample variation and the uncertainty in the nanopillar area.

quasistatically is considerably less than the zero-temperature critical current  $I_{c0}$ . One consequence of this is illustrated in Fig. 3(a), where we show the transition probability of a 100 nm diameter circular 1.2 nm free layer sample subjected to current pulses of increasing amplitude. The shorter the pulse width or the higher the current ramp rate, the larger the bias required to achieve a 50% transition probability during the pulse. Figure 3(b) shows that  $\bar{I}_c$  varies logarithmically with pulse width, as expected for an activated process.

To study in more detail how the thermal activation process affects spin-transfer-driven switching, we varied the current ramp rate for several samples. Results are shown in Fig. 2 for the case of a 300 mA/sec current ramp rate. We find a substantially increased  $\Delta J_c$  compared to 0.1 mA/sec current ramp rate. Following [24–27], the activation barrier is assumed to be of the form  $U(J) = U_0(1 - J/J_{c0})^{c_1}$ , where  $J_{c0}$  is the zero-temperature critical-current density,  $c_1$  is a constant, and  $U_0$  depends on the physical parameters of the nanomagnet. For a given ramp rate, this states that the finite-temperature mean critical-current density is

$$\bar{J}_c(r, T) = J_{c0} \left\{ 1 - \left[ \frac{k_B T}{U_0} A(r, T) \right]^{1/c_1} \right\},$$

$$A(r, T) = \ln \left[ \frac{c_1 k_B T |J_{c0}|}{\tau_0 U_0 |r|} \left( \frac{|J_{c0}|}{|J_{c0} - \bar{J}_c|} \right)^{c_1 - 1} \right].$$

Here  $r$  is the current ramp rate and  $\tau_0^{-1}$  is the fluctuation attempt rate. Since  $A(r, T)$  depends only weakly on its

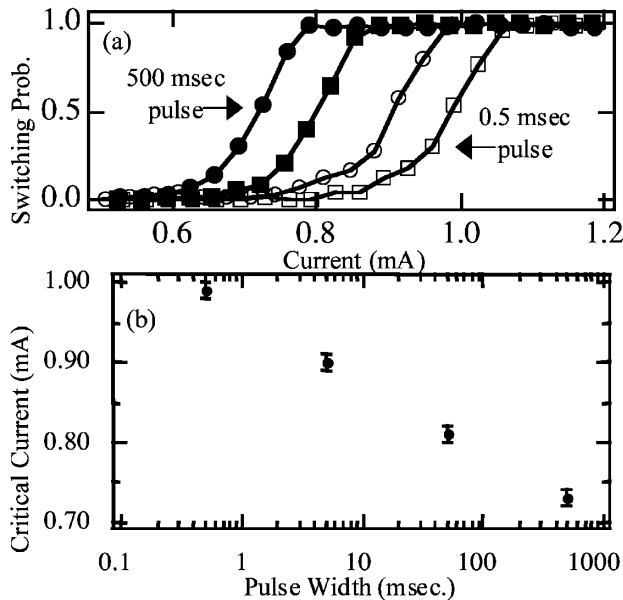


FIG. 3. (a) Critical current  $I_c^+$  for switching to the antiparallel state as measured as a function of pulse duration for a 100 nm diameter circular Co 4.8 nm/Cu 6 nm/Co 1.2 nm trilayer. (b)  $I_c$  (50% switching probability) from (a) as a function of pulse duration.

variables, a dependence of  $A$  on  $t_{\text{Free}}$  would not be noticeable in the data. However, if  $U_0$  scaled with  $t_{\text{Free}}$ , then  $\bar{J}_c(r_1, t_{\text{Free}}) - \bar{J}_c(r_2, t_{\text{Free}})$  would not scale linearly with  $t_{\text{Free}}$ . For our two ramp rates, both  $\bar{J}_c(r, t_{\text{Free}})$  and  $\bar{J}_c(r_1, t_{\text{Free}}) - \bar{J}_c(r_2, t_{\text{Free}})$  vary linearly with  $t_{\text{Free}}$ , indicating that  $U_0$  for current-induced switching is effectively independent of  $t_{\text{Free}}$ .

This lack of dependence of the activation barrier on  $t_{\text{Free}}$  is somewhat unexpected. We note that an estimate of  $U_0$  obtained from the pulse-rate dependence of  $J_c$  (Fig. 3) indicates that the activation barrier is relatively low,  $\sim 1.5$  eV (assuming  $c_1 = 1.5$ ); much less than expected for the coherent reversal of a single domain nanomagnet with the volume of the free layer [11,25–27]. This may be indicating that the dynamics for the initiation of spin-transfer-driven magnetic reversal in these samples is more complicated than activation over a single barrier. But regardless of the explanation, thermal fluctuations do not appear to be affecting the determination of the functional dependence of  $J_c$  on  $t_{\text{Free}}$ .

In the original spin-transfer model [1–5], a spin torque arises from spin-dependent scattering (reflection) at a paramagnet/ferromagnet interface. This transfers transverse angular momentum (spin) to the magnetic moment, exerting a torque that, once it is strong enough to overcome the damping, can cause the moment to reverse its direction. In this spin-dependent reflectivity model, for zero offset fields,  $\Delta J_c \propto t_{\text{Free}}$  [25–27], since the damping and anisotropy forces that resist switching scale with  $t_{\text{Free}}$ , but the spin torque per unit current that drives the switching does not.

Some alternative models of spin-current switching treat the spin transport as a semiclassical diffusion problem and consider the nonequilibrium spin accumulation that develops as result of current (spin) flow. Heide and co-workers consider the longitudinal spin accumulation that is expected to develop in both the fixed and free layer and to extend over the spin-relaxation length [7]. This is argued to act as an effective field, proportional to the current, with switching occurring when this field exceeds  $H_{c,\text{Free}}$ . In this effective field model, the result is  $\Delta J_c \propto H_{c,\text{Free}} t_{\text{Free}} / t_{\text{Fixed}}$ . Though the prediction that  $\Delta J_c \propto t_{\text{Free}}$  is consistent with observations, the prediction that  $\Delta J_c \propto 1/t_{\text{Fixed}}$  is not. When  $t_{\text{Fixed}}$  was increased by a factor of 4 for samples with a 2.4 nm free layer,  $\Delta J_c$  varied by no more than our present uncertainty ( $< 10\%$ ). In addition, sample to sample variations yielded values of  $H_{c,\text{Free}}$  which differed by up to a factor of 2 with no significant difference in  $\Delta J_c$  ( $< 10\%$ ).

Another recent model [8] focuses on the transverse spin accumulation that is assumed to develop at the surface of the free layer and decay over a characteristic length  $\lambda_j$  as the injected electrons diffuse into the ferromagnet and which acts as both an effective field and a spin torque. The predicted result is  $\Delta J_c \propto t_{\text{Free}}$  for  $t_{\text{Free}} \gg \lambda_j$  and  $\Delta J_c \approx \text{const}$ , for  $t_{\text{Free}} < \lambda_j$ , where  $\lambda_j$  is predicted

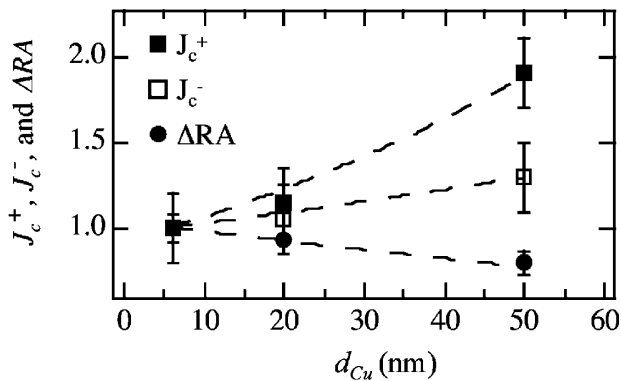


FIG. 4. Normalized critical current density  $J_c^-$  (open squares),  $J_c^+$  (closed squares), and magnetoresistance  $\Delta RA$  (closed circles) as a function Cu spacer layer thickness  $d_{Cu}$ . The dashed lines are fits to the data (see text).

to be on the order of 2 nm. The data of Fig. 2 indicate that  $\lambda_J \ll 1.2$  nm, i.e., much less than the estimates of Zhang *et al.* [8].

We have also examined the effect that the spacer layer thickness  $d_{Cu}$  has on  $\lambda_J$  and  $\Delta RA$ . As  $d_{Cu}$  becomes comparable to the spin-relaxation length  $\lambda_s$ , we would expect an increase in both  $J_c^+$  and  $J_c^-$  and a decrease in  $\Delta RA$  due to the reduction in the polarization of the current incident on the free layer. Figure 4 shows  $J_c^+$ ,  $J_c^-$ , and  $\Delta RA$  as a function of  $d_{Cu}$  for nanopillars where the  $t_{Fixed} = 8.0$  nm and the  $t_{Free} = 2.0$  nm. Note that, between  $d_{Cu} = 6$  and 50 nm, the  $\Delta RA$  decreases only by 23% and  $J_c^-$  increased only by 30% while the  $J_c^+$  increases by 90%. If the relaxation rate is not too high, then  $\Delta RA(d) = \Delta RA(0)e^{-d/\lambda_s}$  [28,29], where  $d$  is the distance traveled in the Cu layer. Fitting this to the  $\Delta RA$  data yields  $\lambda_s = 190 \pm 20$  nm. For spin-transfer switching  $J_c \propto g(\theta)^{-1}$ , where  $g$  is the spin-torque efficiency. As more spin relaxation is introduced into the spacer layer, the spin-torque efficiencies will become smaller, thus increasing  $J_c$ . In the spin-dependent reflectivity model, to leading order, the spin-torque efficiency for a finite spacer layer scales with  $(e^{-d/\lambda_s})$ . For the transition from antiparallel to parallel alignment ( $\theta = \pi$ ),  $d = d_{Cu}$ . But for the parallel to antiparallel transition ( $\theta = 0$ ), spin-down electrons flow from the free layer to the fixed layer, whence they are reflected back to the free layer to exert the torque resulting in antiparallel alignment [2]. Thus, here  $d = 2d_{Cu}$ . Fitting the  $J_c$  data with this modification of the spin-dependent reflectivity model, we obtain a RT Cu spin-relaxation length of  $\lambda_s = 170 \pm 40$  nm using the  $J_c^-$  data and  $\lambda_s = 140 \pm 30$  nm using the  $J_c^+$  data. If we do not take into account the doubled distance that the reflected electrons take to affect the parallel to antiparallel transition, we obtain  $\lambda_s = 70 \pm 20$  nm from the  $J_c^+$  data, which is not in agreement with the  $\Delta RA$  or  $J_c^-$  data.

In summary, we have studied nanoscale CPP devices consisting of thin-film Co/Cu/Co trilayers of varying

thickness that exhibit reversible spin-current switching of the thinner Co layer. The magnitude of the magnetoresistance of these Co/Cu/Co nanopillar devices is in good accord with recent theoretical and experimental investigations and with the understanding that interfacial spin-dependent scattering (reflection) dominates this magnetoresistance. The spin-transfer critical currents are found to vary linearly with the thickness of the magnetic free layer and to be independent of the thickness of the fixed Co layer. All of these results support interfacial spin-dependent scattering (reflection) as the fundamental cause of spin transfer.

This research was supported in part by ARO and by NSF through the Cornell Center for Materials Research and through the Nanoscale Science and Engineering Center program. Additional support provided by NSF through use of the National Nanofabrication Users Network.

- [1] L. Berger, Phys. Rev. B **54**, 9353 (1996).
- [2] J. C. Slonczewski, J. Magn. Magn. Mater. **159**, L1 (1996).
- [3] Ya. B. Bazaliy, B. A. Jones, and S. C. Zhang, Phys. Rev. B **57**, 3213 (1998).
- [4] X. Waintal *et al.*, Phys. Rev. B **62**, 12317 (2000).
- [5] M. D. Stiles and A. Zangwill, J. Appl. Phys. **91**, 6812 (2002).
- [6] K. Xia *et al.*, Phys. Rev. B **65**, 220401 (2002).
- [7] C. Heide, P. E. Zilberman, and R. J. Elliot, Phys. Rev. B **63**, 064424 (1999).
- [8] S. Zhang, P. M. Levy, and A. Fert, Phys. Rev. Lett. **88**, 236601 (2002).
- [9] J. Z. Sun, J. Magn. Magn. Mater. **202**, 157 (1999).
- [10] E. B. Myers *et al.*, Science **285**, 867 (1999).
- [11] J. A. Katine *et al.*, Phys. Rev. Lett. **84**, 3149 (2000).
- [12] F. J. Albert *et al.*, Appl. Phys. Lett. **77**, 3809 (2000).
- [13] J. Grollier *et al.*, Appl. Phys. Lett. **78**, 3663 (2000).
- [14] J.-E. Wegrowe *et al.*, Europhys. Lett. **45**, 626 (1999).
- [15] M. Tsoi *et al.*, Phys. Rev. Lett. **80**, 4281 (1998).
- [16] K. Bussmann *et al.*, Appl. Phys. Lett. **75**, 2476 (1999).
- [17] J. A. Katine, F. J. Albert, and R. A. Buhrman, Appl. Phys. Lett. **76**, 354 (2000).
- [18] J. A. Katine, A. Palanisami, and R. A. Buhrman, Appl. Phys. Lett. **74**, 1883 (1999).
- [19] S. K. Upadhyay, R. N. Louie, and R. A. Buhrman, Appl. Phys. Lett. **74**, 3881 (1999).
- [20] J. Bass and W. P. Pratt, J. Magn. Magn. Mater. **200**, 274 (1999).
- [21] K. M. Schep *et al.*, Phys. Rev. B **56**, 10805 (1997).
- [22] K. Xia *et al.*, Phys. Rev. B **63**, 064407 (2001).
- [23] M. D. Stiles and D. R. Penn, Phys. Rev. B **61**, 3200 (2000).
- [24] E. B. Myers *et al.*, Phys. Rev. Lett. **89**, 196801 (2002).
- [25] J. Kurkijärvi, Phys. Rev. B **6**, 832 (1972).
- [26] A. Garg, Phys. Rev. B **51**, 15592 (1995).
- [27] W. Wernsdorfer *et al.*, Phys. Rev. Lett. **77**, 1873 (1996).
- [28] W. Park *et al.*, Phys. Rev. B **62**, 1178 (2000).
- [29] T. Valet and A. Fert, Phys. Rev. B **48**, 7099 (1993).